GENERATION OF MULTIPLE COHERENT PULSES IN A SUPERRADIANT FREE-ELECTRON LASER

X. Yang, S. Seleskiy
National Synchrotron Light Source, Brookhaven National Laboratory, Upton, NY 11973, USA
L. Giannessi, Elettra-Sincrotrone, Trieste, S.C.p.A., Basovizza, and ENEA C.R. Frascati, Italy

Abstract

We analyze the structure of the tail of a superradiant pulse, which is constituted by a train of trailing-pulses with decaying amplitudes. We show how a trailing pulse, with phase advance from the leading pulse, is generated at the falling edge of the leading pulse, where the corresponding phase space is deeply saturated and the electrons become de-trapped by the reduced ponderomotive potential. Once the trailing pulse gains enough energy, it generates a second trailing pulse, and the process takes place again. By performing detailed simulations of the resulting electron phase space distribution and the FEL pulse spectral and temporal structure with PERSEO, we confirm that the deformation and re-bunching of the longitudinal phase space create a sequence of pulses.

INTRODUCTION

The free-electron laser (FEL) is a tunable source of coherent radiation, ranging from terahertz (THz) waves to hard X-rays, with the capability for femtosecond time resolution. Progress was made recently in single-pass FELs in moving toward the X-ray region of the spectrum, such as the self-amplified spontaneous emission (SASE) FEL that successfully lased from soft X-rays down to 1.5Å [1,2], and the high-gain harmonic generation (HGHG) FEL [3] pioneered at Brookhaven [4] and now implemented in a facility at Elettra-Sincrotrone Trieste, where FERMI [5,6] provides radiation for user experiments in the VUV and soft X-ray wavelength range. One of the main advantages of the HGHG and laser-seeded FEL over the SASE FEL is that they produce not only transversely, but also temporally coherent pulses. In contrast, SASE radiation starts from the initial shot-noise of the electron beam, so that the resulting radiation exhibits excellent spatial- , but a rather poor temporal-coherence.

In this report, we present numerical evidence for a slippage-dominant superradiance FEL interaction regime, wherein the emitted main FEL pulse is followed by multiple trailing pulses, which we dubbed a "trailing-pulse regime". This dynamic behavior is guaranteed in the circumstance of an ultra-short seed pulse with the power beyond saturation [7,8]; it may be important for the existing and next-generation short-wavelength-seeded FELs, such as the FERMI, and the LCLS-II [9]. A deep understanding and controlling of these regimes are essential for optimizing the power as well as the quality of FEL sources, features demanded by the user communities. Using the Perseo simulation [10], we investigated the behaviors of the seeded FEL, and obtained new insights on the trailing pulse generation that we interpreted in terms of the fragmentation of the most significantly bunched electrons by the main radiation pulse in the longitudinal phase (LPS) into new buckets, which are responsible for the trailing pulses. Here, the term "bucket" denotes the electric field of a radiation pulse that assures longitudinal focusing, thereby constraining the electron's motion to a stable region in LPS.

The mechanism of FEL amplification commonly is analyzed in three steps: energy modulation, exponential growth, and saturation. In the first step, energy is exchanged between the electrons and the radiation, leading to an energy modulation, and further, to a density modulation (microbunching) of the electrons at the resonant wavelength $\lambda_r = \lambda_w(1+K^2/2) / (2\gamma_r^2)$, determined by the electron beam's energy $E_r=mc^2\gamma_r$. $K = eB_w/mck_w$ is the dimensionless undulator parameter, and λ_w, k_w, and B_w are, respectively, the undulator's wavelength, wave number, and magnetic field [11]. Initiating the FEL process with a coherent seed allows to lock in the phase of the microbunches and to achieve an improved temporal coherence. Afterwards, the FEL enters the second evolutionary step: radiation power increases exponentially to the detriment of the electron beam's kinetic energy. The strong energy losses, corresponding to a redshift of λ_r, thereafter disable the electron-radiation field's interaction. In the so called steady state regime, the FEL power reaches a maximum and saturates. However, where pulse propagation effects are considered, the radiation pulse is simultaneously dominated by saturation and slippage [12], and its evolution is characterized by the propagation of a solitary wave with the peak power growing quadratically with time and the pulse length decreasing [12,13,14]. In this regime the main pulse propagates at the velocity of light over the electron current leaving highly bunched electrons after its passage. These electrons in the trailing edge coherently radiate into a new trailing pulse. Here, the trailing-pulse regime can be extended over the entire slippage distance along the electron bunch (Fig. 1). Numerical studies reveal that LPS fragmentation and the formation of new buckets are core ingredients of the trailing-pulse dynamics. In these circumstances, an ultra-short seed-pulse induces microbunching when it slips over the electrons at $v_g \sim c$ [14,15]. Microbunching induces coherent emission of the electrons, forming the main radiation pulse and leaving behind those highly bunched electrons with large energy spread. Due to the energy transfer from electrons to the main radiation pulse, the low-energy part ($p < 0$) carries the larger part of charge (≥70%, obtained by counting the

ISBN 978-3-95450-133-5

number of macro-particles in the low-energy part *vs*. the total number of particles distributed within (-π, π)), and accordingly, a larger bunching coefficient than the high-energy part. It therefore, emits coherent light with a redshift λ_r to become a new trailing pulse. Here, $p = (E-E_0) / \rho \cdot E_0$ is the energy variation with respect to the reference particle E_0, and ρ is the FEL Pierce parameter [16] characterizing the gain of the FEL. This process occurs again in the trailing edge of this second pulse, but with a smaller fraction of trapped charge, due to the increasing energy spread caused by the interaction with the previous pulses (a fraction ≤50%, similarly obtained by counting the particles). Additional trailing pulses are generated.

In this paper we numerically explore the generation and suppression of multiple trailing superradiance pulses in a single-pass FEL amplifiers. We analyze FEL evolution from the viewpoint of electron longitudinal phase-space, showing the relation between the synchrotron oscillation and the structure of the radiation pulse. We support our analysis via simulations obtained with the well-known and established simulation code Perseo [10], employing it to resolve the one-dimensional (1D) FEL model, including the high-order harmonics described by the one-dimension Colson model [11]:

$$\frac{\partial \phi_j}{\partial \bar{z}} = p_j, \qquad 1(a)$$

$$\frac{\partial p_j}{\partial \bar{z}} = -\left[A(\bar{z},\tau)e^{i\phi_j} + c.c.\right] \qquad 1(b)$$

$$\left(\frac{\partial}{\partial \bar{z}} + \frac{\partial}{\partial \tau}\right) A(\bar{z},\tau) = \chi(\tau) b(\bar{z},\tau). \qquad 1(c)$$

Each particle j, j=1…N_e wherein N_e, the total number of electrons in the optical field A, is followed in the phase space using φ_j, the particle's relative phase, and p_j, the particle's relative energy, both normalized to the reference particle. The variables φ_j, p_j, and A are functions of the longitudinal coordinates τ along the electron bunch, and $\bar{z}$ along the undulator. τ is defined within $0 < \tau < L_e$, with L_e the electron bunch's length, and $\bar{z}$ is defined within $0 < \bar{z} < L_w$, with L_w the undulator length. All dimensions are in cooperation length [12,17] units: $l_c = \lambda/4\pi\rho$. χ is the macroscopic electronic-density normalized to 1, and b($\bar{z}$, τ) is the bunching coefficient: $b(\bar{z}, \tau) = (1/N)\ \Sigma e^{-i\varphi j}$. Eq 1(a) and 1(b) describe the particle's dynamics, while Eq. 1(c) includes the pulse's propagation.

SIMULATION

The initial condition for the slippage-dominant superradiance regime is defined more precisely in scaled units using S_{seed} ($=4\pi\rho N_w/L_{seed}$), the ratio of the slippage length to the duration of the seed pulse, S_e ($=4\pi\rho N_w/L_e$), the ratio of the slippage length to the electron-bunch's length [18], and F_{seed} ($=\Delta f_{FWHM}/f_0 \cdot \rho$), the ratio of the seed's spectral bandwidth and the FEL-gain's bandwidth. Within the limit of the short-seed pulse, (S_e<<1) is chosen to have a nearly constant electron current in the simulation window, while (S_{seed}>>1) and (F_{seed}>>1) satisfy the slippage-dominant superradiance condition, where the bandwidth of the seed laser is much larger than that of the FEL gain. Therefore when the seed pulse slips over the electron bunch at $v_g \sim c$, it only microbunches the electrons [13].

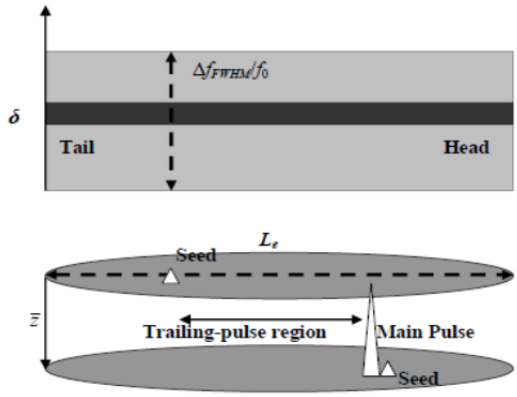

Figure 1: Schematic of the seeded-FEL's initial parameters. $\bar{z}$ is the longitudinal coordinate along the undulator. L_e and $\delta = (E-E_r) / \rho \cdot E_r$ are, respectively, the electron bunch's length and energy detuning. Here, $E_r = E_0$. Δf_{FWHM} is bandwidth of the seed laser.

Eq. 1 is used to simulate the evolution of the FEL in the regime of a long electron bunch and slippage-dominant superradiance, i.e., S_e<<1, S_{seed}>>1, and F_{seed}>>1. Figure 2 illustrates the dynamics of the FEL pulse via 2D diagrams with the longitudinal coordinate along the electron bunch, τ, is plotted in the horizontal axis and the coordinate along the undulator $\bar{z}$ in the vertical axis.

Figure 2(a) depicts the evolution of the FEL into the superradiance regime [15,19,20]. The seed pulse provides microbunching to the electrons when it slips over them at $v_g \sim c$, and maintains its pulse shape in the undulator. Microbunching emits coherent light that grows exponentially to become the main pulse. At the end of exponential growth and in the beginning of superradiance ($\bar{z} \approx 2.6$ in the undulator), the main pulse slips as in the exponential regime ahead of the electron bunch at $v_g \sim c$ instead of at $\sim 3c/(1+2\beta_Z^{-1})$ [21], whilst the length of the pulse decreases and the amplitude increases quadratically with the distance in the undulator. Simultaneously, it induces strong microbunching of the electrons. At a given delay in time, the 1st trailing pulse appears weaker in amplitude compared to the main pulse, similar to the case for the 2nd trailing pulse.

To investigate the origin of multiple trailing pulses, we studied the evolution of the particle's relative longitudinal position (phase). A new trailing pulse appears at the π phase shift with respect to the radiation pulse ahead of it. For FELs, the gain medium consists of relativistic electrons, whilst how well the phase of the microbunches is locked and sheared along the undulator determines the optical field's temporal profile. The phase shift is caused by the energy modulation and FEL's intrinsic dispersion.

ISBN 978-3-95450-133-5

The original reference particle, corresponding to the original bucket center, and also being the reference for the simulation, is fixed in LPS due to the zero energy offset δ_0 (= $(E_0\text{-}E_r) / \rho \cdot E_r$)=0. Here, the bucket center refers to the stable fixed point in the LPS [22]. However, this is not the case for the new reference particle, corresponding to the new bucket center. Rather, it is fixed inside the new bucket but not in the LPS because it has a negative energy-offset (δ<0) with respect to the original reference particle. It drifts toward the direction of the main pulse's tail. Whenever it varies the phase $\Delta\varphi$ across an integer of π, a new trailing pulse appears. $\Delta\varphi_n \approx n\cdot\pi$, n = 1, 2, .., corresponds, respectively, to the 1st, 2nd, .., trailing pulse. As confirmation, Figure 2(b) presents the LPS of the electrons at the newly formed buckets corresponding to the 1st and 2nd trailing pulses at the undulator distance, $\bar{z}$ = 12.8; their phase-changes relative to reference particle are equivalent to ~π and 2π, as indicated by the black dashed lines; this confirms that the π-phase relationship is coincident with the formation of a new trailing pulse. The dephasing of the bunched electrons with the field of the main pulse, causes first the drop of the field amplitude at the trailing edge of the pulse, and then a change of sign of the field which grows with the new phase, shifted of π. The time separation, Δt_n, between the nth trailing pulse and the main pulse is estimated using Eq. 2, derived straightforwardly from Eq. 1(a).

$$\Delta t_n = {n \cdot \lambda_r}\big/{2 \cdot \delta_n \cdot c} \qquad (2)$$

As an example (Fig. 2(c)), the FEL Pierce parameter ρ = 0.004 and λ_r = 800nm, for n = 1, $\delta_1 \approx$ 5.0 (Fig. 2(b)), the Δt_1 calculated using Eq. 2 is ~65fs, which is consistent with the result ~66fs obtained from the simulation.

Further understanding of the physical mechanism behind the trailing-pulse regime also is gained by analyzing the electron's LPS at different positions along the radiation pulse. At the undulator position $\bar{z}$ = 12.8, we obtained the LPS of the electron beam (top), and the overlapping radiation pulse (bottom), as shown in Fig. 2(c). At position A, we show the LPS of the electrons that the seed pulse reaches and they only have the energy modulation. At position B, the effect of the interaction with the optical pulse is evident, such that a strong modulation in energy and density has occurred. On average, the electrons lose energy that is absorbed by the main radiation pulse. At position C, corresponding to the peak of the main pulse, the electrons have reached the bottom of the bucket in phase space, and begin to gain energy from the laser field of the main pulse. Therefore, the power of the laser starts to drop and reaches a minimum at position D, where the corresponding phase space appears deeply saturated and the electrons start to become detrapped by the reduced ponderomotive potential. The strong optical field of the main pulse maximizes microbunching, and also causes a ~5% (ρ = 0.004) spread in the beam's energy. At position E, the electrons are detrapped from the bottom energy after the passage of the main pulse, and are free to start a new process of FEL amplification. Those electrons close to the energy bottom form a new bucket in the series (black dashed circle) that is responsible for generating the new pulse. In addition to the drift in phase brought about by the energy spread and intrinsic dispersion, the majority of the electrons in new buckets arriving at the energy bottom after losing energy to the new pulse generate the peak of the new pulse (see position F). Similar to the main pulse, the electrons already at the bottom of the bucket start to gain energy from the optical field of the new pulse. The energy of the new pulse starts to fall, and reaches a minimum at position G.

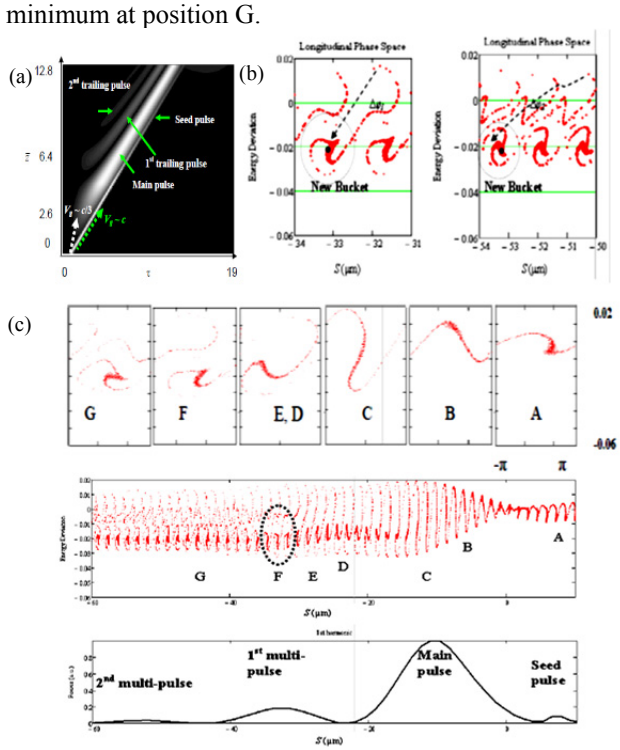

Figure 2: (a) Normalized longitudinal profile of the radiation power along the electron's coordinate, τ, as it evolves along the undulator with coordinate $\bar{z}$. Seed parameters: S_{seed} = 21 (with Gaussian shape, σ_{seed} = 0.26), and F_{seed} = 25 ($\Delta f_{FWHM}/f_0$=0.1, ρ = 0.004). Maximum seed field amplitude at $\bar{z}$ = 0: A_0 = 20. Initially: θ_j uniformly distributed within [-π, π] and p_j following a normal distribution center around zero with standard deviation 0.01%-RMS. L_e = 88, corresponding to S_e = 0.06. (b) At $\bar{z}$ = 12.8 in the undulator, the LPS of the electrons at the positions where the peaks of the 1st (left) and 2nd (right) trailing pulses are. $\Delta\varphi_1 \approx \pi$, and $\Delta\varphi_2 \approx 2\pi$. (c) At $\bar{z}$ = 12.8 in the undulator, the LPS of the electron bunch (top), and the temporal profile of the radiation field along the electron coordinate (bottom). Separation between the main and 1st trailing pulses is ~65fs, and between 1st and 2nd pulses it is ~70fs. The dashed oval signifies the buckets responsible for generating the 1st trailing pulse. In (b) and (c), energy deviation is calculated using the formula $(E\text{-}E_0)/E_0$, and the horizontal axis is the longitudinal position S in units of μm.

ISBN 978-3-95450-133-5

Overmodulation is the signature of local saturation; the bunch slices initially under the peak of the main pulse, modulated via the highest optical field, reach saturation in the undulator, and afterwards are detrapped due to the decrease in intensity at the main pulse's tail edge. Electrons, detrapped from original bucket, shearing in z, and retrapped to new bucket, are responsible for generating the new pulse. Since the electrons carry on their rotation in LPS within the optical pulse's electric field, the process is repeated: Additional pulses still are generated. The radiation power of the trailing pulses continuously degrades to weaker levels, $P_n \approx a \cdot P_{n-1}$ ($a \leq 0.25$), only a fraction of the low-energy portion of the electrons (≤50%) participates in the generation of the new pulse, as shown in Figs. 2(a) - (c). The output power is proportional to the square of the beam's current ($P \sim I^2$) in the superradiance regime. Here, P_n is the FEL power integrated over the n^{th} pulse, and I is the electron-beam's current that contributes to the FEL output.

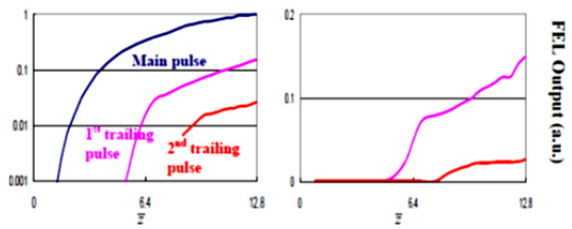

Figure 3: (a) (left) (color online) Evolution of the intensity of the FEL pulse along the undulator calculated using Eq. 1. Intensity integrated over the main pulse (blue), 1st trailing pulse (magenta), and 2nd trailing pulse (red). (b) (right) (color online) Evolution of the FEL pulse intensity normalized by the main pulse along the undulator. 1st trailing pulse (magenta) and 2nd trailing pulse (red).

Figure 3(a) illustrates the evolution of the FEL power (integrated over the radiation pulse) along the undulator for three individual pulses, the main pulse (blue), the 1st trailing pulse (magenta), and the 2nd trailing pulse (red). It confirms that for each radiation pulse, the FEL power first increases exponentially and does not saturate: Its amplification proceeds, power increases as $\bar{z}^2$ [12,14,19,20]. The slippage propels the main pulse forward into the "fresh" electron region that maintains the feeding of the pulse. However, a similar slippage only pushes a trailing pulse forward into the region where the electrons already have lost energy to the radiation pulses ahead of it. Therefore, the output power of each trailing pulse is weaker than that of the pulse ahead of it. Figure 3(b) shows the evolution of the FEL power along the undulator for the 1st and 2nd trailing pulses, normalized by the main pulse. A strong optical field enhances microbunching; therefore, as the intensity of the main pulse rises, that of the 1st pulse increases faster. The undulator $\bar{z}$ position where the FEL process being terminated can be used as a control parameter to choose between moderately higher radiation output (larger $\bar{z}$ (>5.12) is better) or suppression of the trailing pulses after the main pulse ($\bar{z} \leq 5.12$).

In conclusion, depending on the initial conditions (the parameters of the electron beam, the undulator, and the seed laser), a short-pulse-seeded FEL can be driven into various regimes with different temporal- and intensity-behaviors. We addressed a new regime for the deeply saturated slippage-dominant FELs, wherein the multiple trailing superradiance pulses following the main pulse can be either enhanced or suppressed. We showed that trailing pulse generation results from the fragmentation of the LPS into new buckets. Furthermore, we numerically and analytically demonstrated that the formation of a new pulse is closely related to the π phase-change ($\Delta\varphi_n \approx n \cdot \pi$, n = 1, 2, ..) between the original bucket center and the newly developed bucket center. Therefore, the separation Δt between two adjacent pulses can be controlled via the Pierce parameter and (or) the parameters of the seed laser since they both can alter the energy spread of the electron beam. While trailing pulses enhance FEL power by a small amount (<10%), such a phenomenon might spoil the temporal profile of the radiation. We can avoid trailing pulses by modifying the parameters of the electron beam and undulator. We will compare these results with 3D simulations using the FEL code GENESIS 1.3 in the future.

We gratefully acknowledge useful discussions with S. Hulbert, B. Podobedov, and A. Woodhead. We are thankful for support from the NSLS. This work is supported in part by U. S. Department of Energy (DOE) under contract No. DE-AC02-98CH1-886.

REFERENCES

[1] P. Emma (LCLS team), Nature Photonics **4**, 641 (2010).
[2] W. Ackermann *et al.*, Nat. Photon. **1**, 336 (2007).
[3] L. H. Yu, Phys. Rev. A **44**, 5178 (1991).
[4] L. H. Yu *et al.*, Science 289, 932-934 (2000).
[5] E. Allaria *et al.*, Nat. Photonics 6, 699 (2012).
[6] E. Allaria *et al.*, Nat. Photonics 7, 913 (2013).
[7] L. Giannessi *et al.*, Phys. Rev. Lett. **108**, 164801 (2012).
[8] L. Giannessi *et al.*, Phys. Rev. Lett. 110, 044801 (2013).
[9] P. Emma (LCLS team), Nat. Photon. 4, 641 (2010).
[10] L. Giannessi, Proceedings of FEL 2006, (BESSY, Berlin, Germany, 2006), p. 91.
[11] W. B. Colson, IEEE J. Quantum Electron. 17, 1417 (1981).
[12] R. Bonifacio *et al.*, Phys. Rev. A 44, 3441 (1991).
[13] R. Bonifacio *et al.*, Nucl. Instrum. Methods Phys. Res. A 296, 358 (1990).
[14] L. Giannessi *et al.*, J. Appl. Phys. 98, 043110 (2005).
[15] X. Yang *et al.*, Phys. Rev. E 85, 026404 (2012).
[16] R. Bonifacio *et al.*, Opt. Commun. 50, 373 (1984).
[17] W. B. Colson, Phys. Lett. A 59, 187 (1976).
[18] M. Labat *et al.*, Phys. Rev. Lett. 103, 264801 (2009).
[19] D. A. Jaroszynski *et al.*, Phys. Rev. Lett. 78, 1699 (1997).

ISBN 978-3-95450-133-5

[20] T. Watanabe *et al*., Phys. Rev. Lett. 98, 034802(2007).
[21] R. Bonifacio *et al*. Rivista del Nuovo cimento 13, 1 (1990).
[22] S. Y. Lee, Accelerator Physics, World Scientific Publishing Co. Pte. Ltd. (1999).

ISBN 978-3-95450-133-5